

Time-Frequency Source Estimation from MEG data

R.E. Greenblatt^{†1}, A. Ossadtchi^{†2}, L. Kurelowech³, D. Lawson¹ and J. Criado³

¹ Source Signal Imaging, Inc., San Diego CA USA

² St. Petersburg State University, St. Petersburg Russia

³ Scripps Clinic, La Jolla CA USA

Abstract— We extend adaptive beamformers (DICS) [1] and RAP MUSIC [2] to solve the MEG inverse problem in the time-frequency domain for induced and phase-locked components. Using event-related data, we estimate the complex covariances from time-frequency transformed single trials for total power, phase locked, and induced components [3]. We obtain the phase-locked DICS inverse as the difference between the total power and induced solutions. RAP-MUSIC was adapted to constrain the real and imaginary parts of the source space solution. We have verified these methods using simulated data, and validated them with somatosensory and motor MEG data.

Keywords— magnetoencephalography, source estimation, time-frequency, DICS, RAP MUSIC

I. INTRODUCTION

Interest in encephalographic oscillatory events has seen recent renewed attention with experimental and theoretical studies linking coherent multicellular rhythms with cognitive events. Time-frequency analysis overcomes some of the limitations of conventional FFT's, permitting simultaneous time-based and frequency-based analysis. Wavelets have well developed mathematical foundations [4] and have become the method of choice for electromagnetic encephalography (EMEG) time/frequency analysis. Tallon-Baudry et al. [3] introduced the useful distinction between phase-locked and induced components of the averaged oscillatory response. Nonlinearities in estimating the averages obtained from time-frequency transformed data have been an obstacle to the application of conventional source estimation methods to time-frequency transformed data. Greenblatt and Osman [5] and Lin et al. [6] have proposed methods to overcome the non-linearity obstacle by computing single trial distributed source estimates and then averaging in source space. This approach, however, often has unacceptable noise sensitivity for typical experimental conditions, especially at higher frequencies.

Adaptive beamformers have been used to estimate source activity at specified locations for extracranial EMEG data in both the time [7] and the frequency [8] domains. They are

adapted to the data via signal space covariance estimates. Gross et al., [8] proposed the use of an adaptive beamformer to solve the inverse problem in the frequency domain, and later for total power in the time-frequency domain, supporting both source power and coherence estimation [1]. Here, we generalize the adaptive beamformer method in the time-frequency domain, permitting the estimation of inverse solutions to both induced and phase-locked components of the event-related time frequency transformed data. We also show how dipole fitting, using the RAP MUSIC approach [2], may be adapted to all components in the time-frequency domain, extending the results of Sekihara et al [9].

II. METHODS

A. Time-frequency wavelet transforms:

For a single channel time series $s(t)$, we can obtain an estimate of the time-varying frequency component at time t and center frequency f as $z(t, f) = s(t) * w(t, f)$, where '*' represents the convolution operator and $w(t, f)$ is the complex wavelet function [10]. By successive applications at differing center frequencies, a time-frequency map may be constructed, averaged over a set of trials to extract phase-locked and total power components. The induced (non-phase-locked) component may then be obtained as the difference. Due to the linearity of the convolution operation, the resultant complex-valued transform coefficients may be used for source estimation.

B. Covariance matrices

For each trial $1 \leq n \leq N$ and each channel $1 \leq k \leq K$ we compute a set of wavelet coefficients $z_{kn}(t, f)$ parametrized by time t , $t_{min} \leq t \leq t_{max}$ and frequency f , $f_{min} \leq f \leq f_{max}$. For each time-frequency bin (t, f) and for each n -th trial we form vectors $z_n(t, f) = [z_{n1}(t, f), z_{n2}(t, f), \dots, z_{nK}(t, f)]^T$ by collecting the corresponding wavelet coefficients from all channels and use them in computing a set of covariance matrices.

We distinguish three different correlation matrices representing the spatial structure of total power, phase locked

[†] These authors contributed equally to the work in this report.

and induced components. Estimate the total power correlation matrix as

$$\hat{\mathbf{C}}_{sig}^{tot}(t, f) \approx \frac{1}{N} \sum_{n=1}^N \mathbf{z}_n(t, f) \mathbf{z}_n^H(t, f) \quad (1)$$

and the phase-locked correlation matrix as

$$\hat{\mathbf{C}}_{sig}^{lock}(t, f) \approx \left(\frac{1}{N} \sum_{n=1}^N \mathbf{z}_n(t, f) \right) \left(\frac{1}{N} \sum_{n=1}^N \mathbf{z}_n(t, f) \right)^H \quad (2)$$

Under the assumption of independence of phase-locked and induced components in the data, the correlation for the induced component is the difference between the total power and phase-locked component correlations, or

$$\hat{\mathbf{C}}_{sig}^{ind}(t, f) = \hat{\mathbf{C}}_{sig}^{tot}(t, f) - \hat{\mathbf{C}}_{sig}^{lock}(t, f) \quad (3)$$

We define averaged correlation matrices as

$$\hat{\mathbf{C}}_{sig}^{tot,lock,ind} = \frac{\sum_{t=t_{min}}^{t_{max}} \sum_{f=f_{min}}^{f_{max}} \hat{\mathbf{C}}_{sig}^{tot,lock,ind}(t, f)}{(t_{max} - t_{min})(f_{max} - f_{min})}$$

Note, that in that case $\hat{\mathbf{C}}_{sig}^{lock}$ has no longer rank of unity. However, because of likely similarity of correlation matrices corresponding to the t-f bins in the region of interest $\hat{\mathbf{C}}_{sig}^{lock}$ is still significantly rank deficient.

C. Source estimation with scanning beamformers

We propose minor extension of the DICS approach [1] to account for the induced and phase-locked, as well as the total power components by computing invertible data correlation matrices in order to build an estimator for each spatial location for each component separately.

For a specified target location, \mathbf{r} , an adaptive linearly constrained distortionless spatial filter [11] may be constructed as

$$\mathbf{W}_{\mathbf{r}}^T = \left[\mathbf{L}_{\mathbf{r}}^T \hat{\mathbf{C}}_{sig}^{-1} \mathbf{L}_{\mathbf{r}} \right]^{-1} \mathbf{L}_{\mathbf{r}}^T \hat{\mathbf{C}}_{sig}^{-1} \quad (4)$$

$\mathbf{L}_{\mathbf{r}}$ is the forward matrix for the dipole at location \mathbf{r} and two orthogonal orientations in the tangent plane [12]. Note that due to the quasi-static approximation generally used in MEG source estimation [13], the forward matrix is real. $\hat{\mathbf{C}}_{sig}$ is one of the signal space covariance matrices defined by equations 1-3, or an average of several of the same type over a selected time-frequency neighborhood. By combining the lead field vectors of all locations and orientations, we obtain an inverse operator $\mathbf{W} = \{\mathbf{w}_{\mathbf{r}}^T\}$ in which each two columns

correspond to a location representing two orthogonal orientations at location \mathbf{r} . Then given \mathbf{W} and the corresponding $\hat{\mathbf{C}}_{sig}$ we may estimate the source space covariance as

$$\hat{\mathbf{C}}_{src} = \mathbf{W}^T \hat{\mathbf{C}}_{sig} \mathbf{W}$$

The 2×2 diagonal submatrices of $\hat{\mathbf{C}}_{src}$ may be used as an estimate of the voxel-wise source space power, either by computing the trace or using the largest eigenvalue. The results may be presented either directly or as the voxel-wise ratio of estimated activations between two conditions (e.g., pre- vs. post-stimulus) [8].

Equation 4 may be applied directly for the total power and induced covariances. However, the phase-locked covariance is significantly rank-deficient, and therefore non-invertible. We propose to resolve this by estimating the source distribution underlying the the phase-locked component as the difference between total power and induced source space estimates. To do so, for each voxel we first compute $\hat{\mathbf{C}}_{src}^{tot}$ and $\hat{\mathbf{C}}_{src}^{ind}$ using the corresponding covariance matrices. Then, we compute source estimate for the phase-locked component as the larger eigenvalue of the diagonal submatrices of the difference matrix $\hat{\mathbf{C}}_{src}^{lock} = \hat{\mathbf{C}}_{src}^{tot} - \hat{\mathbf{C}}_{src}^{ind}$

Taken together, both the diagonal and the off diagonal 2×2 submatrices of $\hat{\mathbf{C}}_{src}^{locked}$, $\hat{\mathbf{C}}_{src}^{tot}$, $\hat{\mathbf{C}}_{src}^{ind}$ may be used to estimate source space coherence between the corresponding locations.

D. Time-frequency RAP MUSIC

RAP MUSIC as applied to neurophysiological data was developed originally to fit dipoles to real-valued covariance matrices [2]. MEG-MUSIC applied to total power was described in [9]. Although the original MUSIC algorithm was described for complex-valued matrices obtained from e.g., multisensor radar signals, the physical basis of the MEG signal differs from the radar case in a significant way. The complexity in the radar case arises from the necessity to model finite propagation delays. In EEG/MEG source modeling we use the quasi-static approximation [13] that implies the absence of delays in propagation of the electromagnetic field from neuronal generators to sensors. Real and imaginary parts of the wavelet coefficients carry complimentary information about the *temporal* structure of source activations and should be used concurrently in order to estimate the *spatial* parameters of the source.

To find the source dipoles we first perform SVD of the complex covariance matrix corresponding to the component of interest, i.e. $\mathbf{C}_{sig}^{tot,lock,ind} = \mathbf{U} \mathbf{S} \mathbf{V}^T$, yielding complex left singular matrix \mathbf{U} and real diagonal matrix $\mathbf{S} = \text{diag}(s_i)$, $1 \leq i \leq K$. Based on user specified threshold on percentage of unexplained variance, we find the effective rank R of the

averaged covariance matrix. Since the spatial information in the wavelet-transformed signal is contained in both real and imaginary parts of the covariance matrix we turn R complex columns of U into a new $K \times 2R$ quasi-data matrix D by filling its columns with weighted by the corresponding singular values real and imaginary parts of columns of U , i.e.

$D = [s_i \Re(\mathbf{u}_i) s_i \Im(\mathbf{u}_i)] \forall 1 \leq i \leq R$. We then use this newly created quasi-data matrix as an input to RAP-MUSIC algorithm with user-specified signal subspace rank parameter that we increase by a factor of 2 to account for the complexity of the original covariance matrices.

E. Simulations

To verify the methods, we simulated two dipoles in a virtual spherical head model, using sensor locations corresponding to a 148 channel first order magnetometer system. Both of the dipoles were active at 75 Hz frequency following an event marker, but differed in that the dipole on the left side was phase-locked to the event, while the dipole on the right side was phase-randomized with respect to the event. 70 trials were averaged in the time-frequency domain. The total power, phase locked and induced components were analyzed using both DICS and RAP MUSIC. The results are shown in Figure 1.

F. Experimental data

We used magnetic field data from simple sensory and motor paradigms to evaluate the source estimation methods, since the paradigms we selected make strong predictions for the anatomical regions of interest [14]. In the case of the motor protocol, we predicted that we would observe beta desynchronization arising from contralateral primary motor cortex [15]. For the sensory evoked field paradigm, we predicted that we would observe a phase-locked activity shortly after the stimulus arising from contralateral primary sensory cortex. In addition, we felt confident that we could identify central sulcus anatomically from the MRI for this subject, and thus infer that primary motor cortex lay anterior to and primary sensory cortex lay posterior to the central sulcus.

Data acquisition: Magnetic field data were acquired from a healthy adult male volunteer using a 148 channel first order magnetometer system (Magnes 2500, 4D Neuroimaging, Inc, San Diego CA). The data were acquired in two separate sessions, once to acquire somatosensory evoked field data, and on another occasion to acquire voluntary motor data. A volumetric set of T1-weighted structural MRIs were also available for this subject. Protocols were approved by the Scripps Clinic Institutional Review Board. Magnetometer sensor locations were determined with respect to head fiducial points

using 4D Neuroimaging software and a Polhemus (Colchester VT) 3D digitizer. The sensors were coregistered to the structural MRI using EMSE Suite v5.3 (Source Signal Imaging, Inc., San Diego CA). EMSE Suite software was used for all subsequent analysis steps, as well.

Motor paradigm: In the voluntary motor paradigm, the subject was instructed to squeeze his left hand into a fist, then extend his hand back to the resting position, approximately once every 3 seconds. A pair of electrodes were placed on the skin over the flexor muscles of the left forearm and the EMG signal was recorded in parallel with the MEG. A total of 42 successive squeezes were used for subsequent analysis. In order to determine movement onset, the EMG was Hilbert transformed to obtain the envelop. The onset was determined by visual inspection of the filtered EMG signal as the earliest time at which the envelop exceeded the background. The results of analysis are presented in Figure 2

Somatosensory paradigm: Airpuff somatosensory stimuli were presented every 330 msec. to the left index finger of an adult male. Data were time-frequency transformed and averaged to obtain the phase-locked component of the evoked field. A RAP MUSIC dipole fit to the phase locked average was calculated for the interval [0.04-0.6 sec, 25-50 Hz], and the results are shown in Figure 3, where the single dipole fit is near or slightly posterior to right central sulcus.

III. RESULTS

Simulations: Simulations: The results for DICS are shown in Figure 1, and described here for both DICS and RAP MUSIC. For the total power case, both DICS and RAP MUSIC correctly identified both dipole locations and orientations, within the 1cm grid tolerance for DICS, and with approximately 1mm rms location error for RAP MUSIC. For the

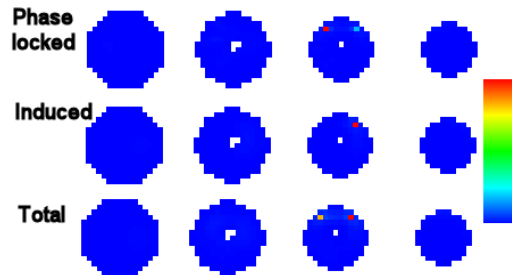


Figure 1: Source estimates from simulated data are shown using DICS for the three components. DICS found both components for the total power case at the correct dipole locations. For the phase-locked case, DICS finds the correct dipole, but also sees a contribution from the non-phase-locked location. In the induced case, DICS finds a single dipole at the correct location. DICS maps computed as pSPM and plotted on axial slices, 1cm separation.

phase-locked case, RAP MUSIC finds one dipole at the correct location for high (0.99) subspace correlation threshold, and two dipoles (at both simulated locations) for lower (0.95) threshold. Similarly DICS finds two locations in the phase-locked case, with a stronger source estimate for the (correct) phase-locked dipole. The appearance of two sources in the phase-locked estimates may be attributed to incomplete averaging, with the phase-randomized signal leaving a residual in the phase-locked transform. For the induced case, both methods correctly identified the (single) phase-randomized dipole source. In this case, RAP MUSIC obtains the same result at either high or low threshold. *Experimental data:* DICS localized primary motor cortex from the β -desynchronization induced correlation, shown in Figure 2. RAP MUSIC localized primary somatosensory cortex from phase-locked SEF data, shown in Figure 3.

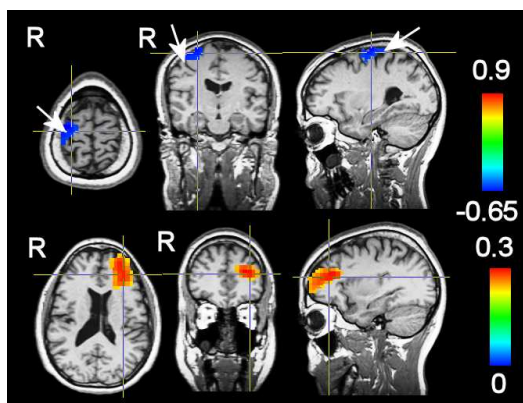


Figure 2: (top) Induced DICS $\log(pSPM)$ inverse is shown for selected interval (0.05-0.18 sec, 17-24 Hz). The right central sulcus (arrow) was identified as the first sulcus anterior to the ascending branch of the right cingulate sulcus, which may be identified unambiguously in successive sagittal slices. (bottom) A brain voxel was chosen near the maximum of the event related desynchronization in right primary motor cortex, and coherence was estimated for the remaining brain voxels. The maximum coherence was observed in left dorsolateral prefrontal cortex.

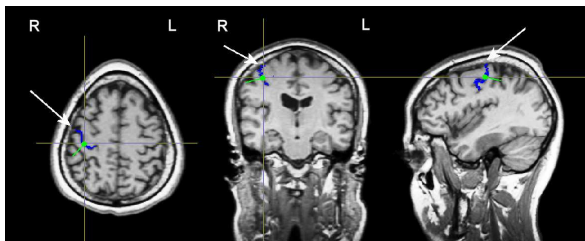


Figure 3: RAP MUSIC fit a dipole (signal space correlation threshold 0.95, rank = 2) to SEF data. One dipole was found at the location shown. The right central sulcus (arrow, sulcus shown in blue) was identified as the first sulcus anterior to the ascending branch of the right cingulate sulcus, which may be identified unambiguously in successive sagittal slices.

IV. CONCLUSIONS

We report a modest, but potentially useful, extension to existing MEG source estimation methods. By estimating distributed (DICS beamformer) and discrete (RAP MUSIC) methods to total power, phase-locked, and induced components of time-frequency transformed MEG data, we can address a broader range of questions than previously, for example, attributing brain sources to event-related synchronization, while minimizing contributions from phase-locked components.

Our results support the conclusion that time-frequency source estimation from MEG data is feasible for all components, using either distributed or discrete methods. They also suggest a potential clinical application in the localization of primary motor cortex using DICS-based source estimation of the β -desynchronization obtained during a voluntary motor task. Additional studies will be required to validate the clinical utility of this approach.

REFERENCES

1. J Gross, F Schmitz, I Schnitzler, et al. Modulation of long-range neural synchrony reflects temporal limitations of visual attention in humans *Proc Natl Acad Sci (US)*. 2004;101:13050-13055.
2. JC Mosher, RM Leahy. Source localization using recursively applied and projected (RAP) MUSIC *IEEE Trans Sig Proc*. 1999;47:332-340.
3. C Tallon-Baudry, O Bertrand, C Delpuech, J Pernier. Stimulus Specificity of Phase-Locked and Non-Phase-Locked 40 Hz Visual Responses in Human *J. Neuroscience*. 1996;16:4240-4249.
4. Y Meyer. *Wavelets: algorithms and applications*. Philadelphia: SIAM 1993.
5. RE Greenblatt, A Osman. Wavelet-based Neuroelectromagnetic Source Estimation *NeuroImage*. 2003;19:CD-ROM.
6. F-H Lin, T Witze, MH Hämäläinen, AM Dale, JW Belliveau, SM Stufflebeam. Spectral spatiotemporal imaging of cortical oscillations and interactions in the human brain *NeuroImage*. 2004;23.
7. SE Robinson, DF Rose. *Current source image estimation by spatially filtered MEG:761-765*. Amsterdam: Excerpta Medica 1992.
8. J Gross, J Kujala, M Hamalainen, L Timmermann, A Schnitzler, R Salmelin. Dynamic imaging of coherent sources: Studying neural interactions in the human brain *Proc Natl Acad Sci USA*. 2001;98:694-699.
9. K Sekihara, S Nagarajan, D Poeppel, Y Miyashita. Time-Frequency MEG-MUSIC Algorithm *IEEE Trans Med Imaging*. 1999;18:92-97.
10. R Kronland-Martinet, J Morlet, A Grossmann. Analysis of sound patterns through wavelet transforms *Intl. J. Pattern Recog. Artificial Intelligence*. 1987;1:273-302.
11. RE Greenblatt, A Ossadtchi, ME Pflieger. Local Linear Estimators for the Bioelectromagnetic Inverse Problem *IEEE Trans Signal Proc*. 2005;53:3403-3412.
12. JC Mosher, RM Leahy, PS Lewis. EEG and MEG: Forward Solutions for Inverse Methods *IEEE Trans BME*. 1999;46:245-259.
13. Lütkenhöner B. Frequency-domain localization of intracerebral dipolar sources *EEG. Clin. Neurophysiol*. 1992;82:112-118.
14. A Papanicolaou. *Clinical Magnetoencephalography and Magnetic Source Imaging*. Cambridge: Cambridge Univ. Press 2009.
15. G Pfurtscheller, Silva FH Lopes. *Event-Related Desynchronization*. Amsterdam: Elsevier 1999.